AN IMPROVED EFFICIENCY PERMANENT MAGNET BRUSHLESS DC MOTOR PV PUMPING SYSTEM

A. MOUSSI, A. TORKI,

ABSTRACT

This paper presents the optimal operation of a photovoltaic pumping system. The operation of a permanent magnet brushless DC motor driving a centrifugal pump is investigated. The motor is controlled through a hysteresis current loop and an outer speed loop with a PI type controller. The proportional and integral gains are set to their optimal values. In order to optimise the overall system efficiency, a Maximum power point tracker is also used. Simulation is carried out by formulating the mathematical model for the photovoltaic source, MPPT, motor and pump load. System performances are investigated under different levels of solar insolation. The effectiveness of the proposed controller is also demonstrated.

I. INTRODUCTION

It is well known that the sun provides almost all the energy needed to support life. On average, the earth receives about 1.2×10^{15} KW of solar power. The challenge for a sustainable future is to tap a tiny fraction of this energy to supply the relative modest demands of human activities. Probably the most elegant way known of doing this is to convert it straight into electricity using solar cells.

The first efficient solar cell was made by Bell Laboratories in 1954. Recent advances in solid state technologies has given a boost to solar cells implementation. High efficiency solar cells are nowadays available with acceptable price. The PV modules production is rising steadily and is expected to reach 10GW by 2010 if the current trends continues [1].

Due to the initial installation price, one has to properly size and optimise the system operation. Most of the research work concentrates on the optimal use of photovoltaic generators which exhaust about 60 to 80% of the global price depending on whether storage means are used or not. The PV systems can be operated as a stand-alone, hybrid or grid connected systems. The first schemes found a wide application in remote regions to meet small, but essential electric power requirement such as water pumping systems [2-5].

Early studies have concentrated on ways of sizing, matching and adapting PV pumping systems since a proper match between the installed capacity with the

isolated load is essential to optimise such installations. Various studies have been done on the choice of the drive system, which suits PV source, type of pumps to use and ways to control and optimise the whole system [6-17]. This was firmly related to the existing technologies

At the early stage, only DC motors were used to drive pumps. Direct coupling of series, shunt, and separately excited DC motor PV pumping systems were studied [06-10]. Steady state and transient performances were considered. It was found that the overall performances are totally different of those obtained when these motors are connected to a constant voltage source. The separately exited and permanent magnet motors were found the more suitable for PV system, the PM motor offering a high power/weight and torque/current ratio. Recent implementation showed that the PM motors are well suited for PV pumping, [12-14,33]. They features high level dynamics, fast response, and high efficiency which lend them naturally suited for PV pumping systems mainly for low power.

Similar work was curried out later feeding motors through a DC/DC converter [8, 10-14] for a better adaptation of the load to the source. Steady state and starting current and torque ratios, efficiency improvement, and control implementation were analysed. The use of the adaptation techniques not only optimises the output power from the PV generator but also improves motor characteristics such as starting torque and steady state parameters.

Many types of power converters are being used such buck, boost and buck boost chopper. Recent research has dealt with most of theses converters in order to find the one most compatible with the PV conversion system in matter of power efficiency [29-32]. It was stated that the boost converter is the most convenient for maximum power tracking. Furthermore, if the required output voltage is less than the generated one, it was recommended to use a two stage conversion unit, boos+step down converter [29].

For PV pumping, two types of pumps are widely used: the volumetric pump and the centrifugal pump. It is found the energy utilisation of the PV generator by the centrifugal pump is much higher than by the volumetric pump. The operation of the former takes place for longer periods even for low insolation levels and its load characteristic is in closer proximity to the max power locus of the generator [7,15-17].

Later, AC motor were introduced mainly for larger powers [?]. Steady state and transient characteristics were considered [17-19]. The motor characteristics are severely affected by the PV source which was considered as a current generator with dependent voltage source. Two way were adopted, either to optimise the power of the generator or the motor efficiency. Different relationship was deduced in each case. However it was found that if maximum motor efficiency is aimed for, the PV generator operates efficiently in a small range only and the period of solar utilisation is unacceptably reduced ($\cong 50\%$). For such applications, an inverter should be included in order to perform the DC/AC conversion stage [17-20]. Mainly, the six steps quasi-square wave

inverter was used. Of course, a PWM inverter yields better waveforms at no real increase in cost.

For small appliances, and in parallel with the recent advances in power electronics, new types of pumps are used such as the vibratory pump, used in conjunction with DC/AC resonant converters. [31]

This paper presents a hysteresis current controller for optimal operation of a brushless PM DC motor PV pumping system with an outer speed loop. Maximum power tracker is also included to optimise the PV generator efficiency as well. The mathematical models for individual blocks like PV generator, motor, pump, ..etc are presented. Simulation results and conclusion follow thereafter.

The combined system mainly consists of the Solar cell array generator, DC/DC converter, PMBLDC motor coupled to a centrifugal pump as shown in Fig.1.
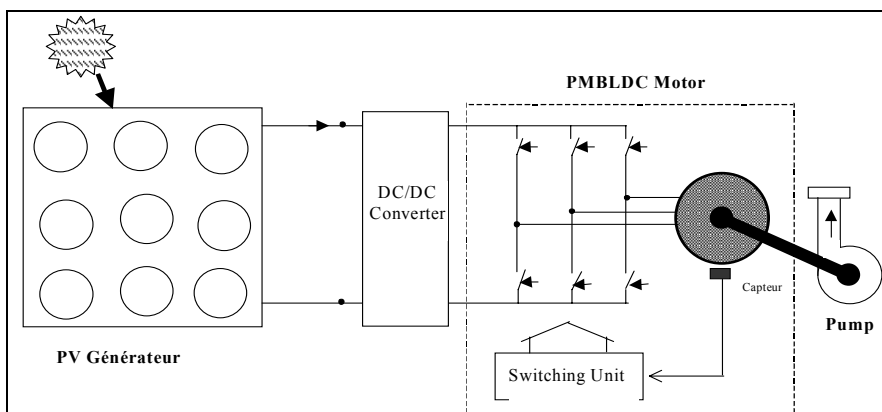

Fig 1 : The PV Scheme Structure

II. PV GENERATOR MODEL

The PV scheme structure is shown in Fig.1. It consists of solar cell Array, DC/DC converter and a PM brushless DC motor coupled to a centrifugal pump load.

The solar cell represents the fundamental power conversion unit of a PV system. For practical use, they are usually assembled into modules. About 36 cells are typically interconnected in series in order to give a charging voltage for a 12V battery. For a high power requirement, the modules are interconnected in series/parallel to form a DC power-producing unit array known as an array or PV generator.

The equivalent circuit of a PV Module is shown in Fig.2. In normal application, resistance R_{sh} is assumed high and can be neglected [5]. Therefore the IV characteristic for a generator formed by N_s series modules and N_p parallels ones, is given by :

$$I = I_p - I_o[\exp\left(\frac{V + R_s I}{V_{th}}\right) - 1]$$ (1)

where I_p is the photovoltaic current I_o the reverse saturation diode current R_s the series resistance and V_{th}, the thermal voltage given by

$$V_{th} = \frac{AkT}{q}$$

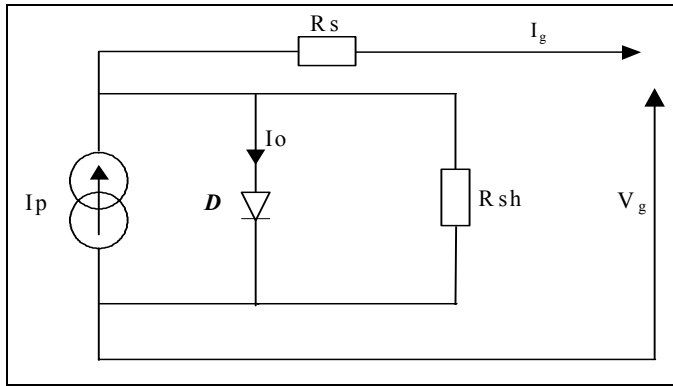where A is the completion factor, K Boltzman constant, T absolute temperature and q the electron charge

Fig 2 : Equivalent Circuit of the PV generator

Equation (1) is used to obtain the output characteristics of the PV generator. The main characteristics which identify a PV generator are shown in Fig.3. As it is clearly seen, the I-V output characteristic of a PV module is highly non-linear. It behaves as current source for the left zone and as a voltage source in the right zone. The output power in theses regions is far below the optimal values which could be generated if the solar array works around the knee of the I-V characteristic. The effect of solar insolation and temperature is shown on Fig.4:a-b respectively. The simultaneous effect of both is also shown in Fig.4:c-d since, practically, any rise in solar insolation level is accompanied by an increase in temperature.

The simplest way to achieve a PV pumping system is to perform a direct coupling of the load, i.e. motor-pump, to the PV source [6-11]. This is the cheapest solution. However, even if the size of the PV generator is initially optimised, it is shown that the efficiency falls heavily if temperature, insolation or drive parameters change.

In order to optimise the output power, i.e. to track the maximum power of the PV generator, various Maximum Power Point Tracker techniques or MPPT are used such as: fixed voltage control, power calculation , incremental conductance etc …[27].
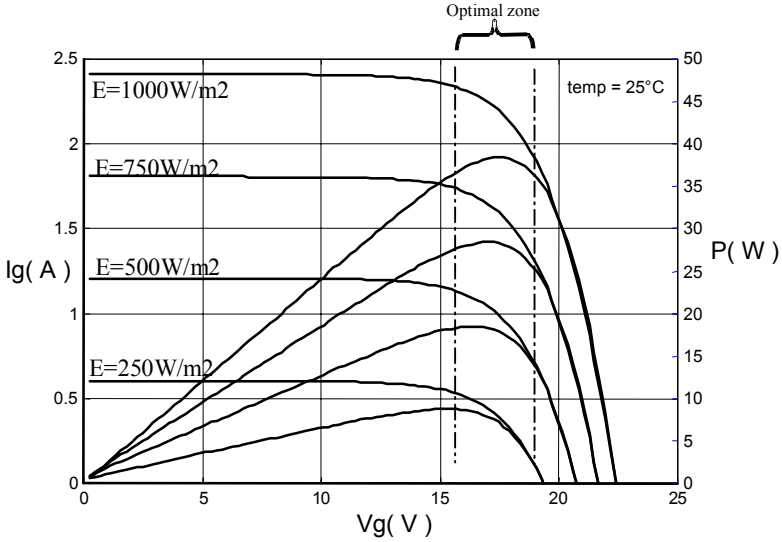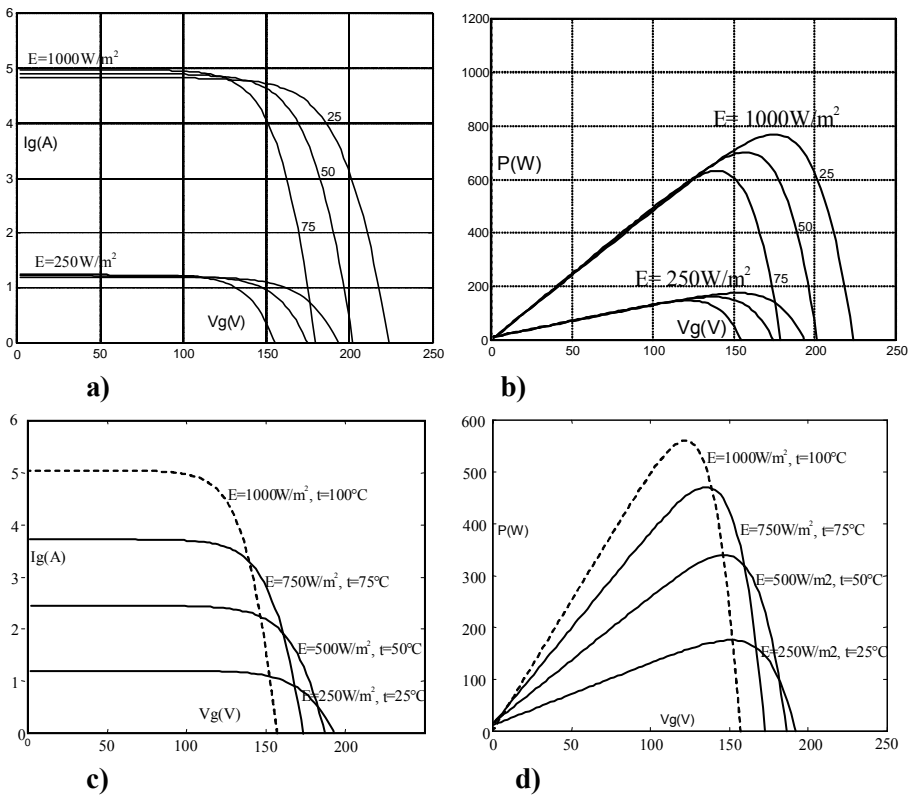
Fig.3 : Photovoltaic module characteristics

a)

b)

c)

d)

Fig.4 : Photovoltaic generator characteristics as a function of
- a-b: Solar insolation (250-1000 W/m^2) and temperature (25,50 and 75° C)
- c-d: Solar insolation and temperature simultaneously

Several ways have been suggested to implement MPPT`s using analogue circuits, digital electronics through microcomputer, DSP`s and single ship micropcontroller. Modern control approaches, such as Fuzzy Logic, Neural Network and robust control are nowadays used to fulfil the function of tracking the maximum power point of hybrid and grid connected PV system. [20-28].

III. PERMANENT MAGNET BRUSH-LESS DC MOTOR MODEL

The simplified schematic of the motor is shown in Fig.5. Since the brushless PM DC motor has a trapezoidal electromotive force, the use of Park transform is not the best approach in modelling the machine. Instead the natural approach is used where the e.m.f is generated with respect to rotor position [12,14,18,23]. The operating sequences of the machine can be subdivided into six cycles with respect to rotor position. Fig 6 shows the back emf and current waveforms for phase a, b and c and Table.2 summarises all the sequences.
The electric part of the motor can be described by [17, 19, 24].:

$$V_{an} = Ri_a + p\lambda_a + e_a \tag{2}$$

$$V_{bn} = Ri_b + p\lambda_b + e_b \tag{3}$$

$$V_{cn} = Ri_c + p\lambda_c + e_c \tag{4}$$

with
$$V_{an} = V_{a0} - V_{n0} \tag{5}$$

$$V_{bn} = V_{b0} - V_{n0} \tag{6}$$

$$V_{cn} = V_{c0} - V_{n0} \tag{7}$$

where   R : per phase stator resistance $i_{a,b,c}$: phase currents of phases a ,b and c. $\lambda_{a,b,c}$: total flux linkage of phases a, b and c. p : Laplace operator
The flux expressions are given by the following expressions:

$$\lambda_a = L_s i_a - M(i_b + i_c) \tag{8}$$

$$\lambda_b = L_s i_b - M(i_a + i_c) \tag{9}$$

$$\lambda_c = L_s i_c - M(i_a + i_b) \tag{10}$$

where   Ls : the self inductance and M : the mutual inductance.
and
$$i_a + i_b + i_c = 0 \tag{11}$$

Therefore by substituting Eq.10 in Eqs 7, 8 and 9 :
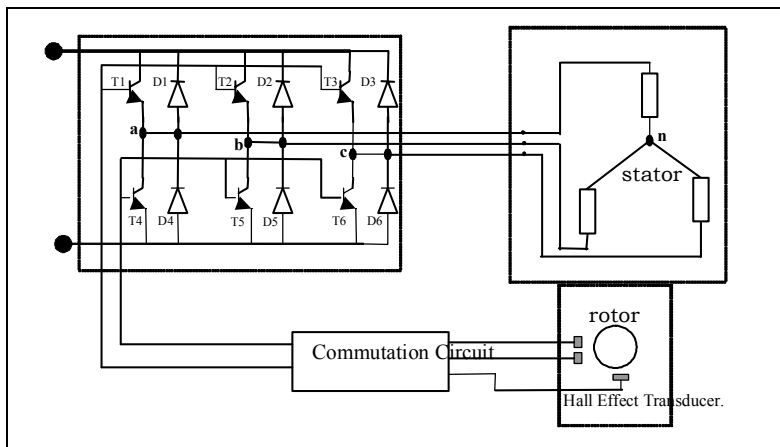$$\lambda_a = i_a(L_s + M) \tag{12}$$

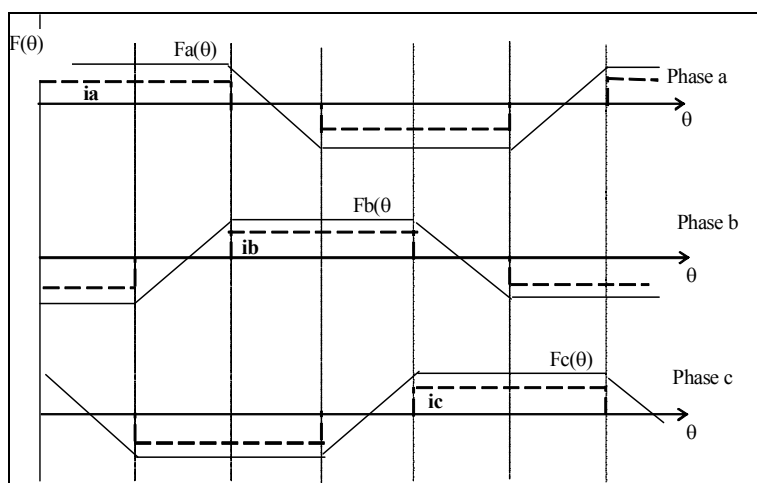*Fig.5 : Brushless PM DC motor and its drive*

Fig.6 : Back e.m.f and current waveforms

$$\lambda_b = i_b(L_S + M) \tag{13}$$

$$\lambda_c = i_c(L_S + M) \tag{14}$$

From the electrical equations 1,2 and 3, the following system is obtained

$$\begin{bmatrix} V_{an} \\ V_{bn} \\ V_{cn} \end{bmatrix} = \begin{bmatrix} R & 0 & 0 \\ 0 & R & 0 \\ 0 & 0 & R \end{bmatrix} \begin{bmatrix} i_a \\ i_b \\ i_c \end{bmatrix} + p \begin{bmatrix} L_{eq} & 0 & 0 \\ 0 & L_{eq} & 0 \\ 0 & 0 & L_{eq} \end{bmatrix} \begin{bmatrix} i_a \\ i_b \\ i_c \end{bmatrix} + \begin{bmatrix} e_a \\ e_b \\ e_c \end{bmatrix} \tag{15}$$

with $L_{eq} = L_S + M$

from this system, the decoupled phase equations are obtained and the explicit current equations are given by :

$$p \begin{bmatrix} i_a \\ i_b \\ i_c \end{bmatrix} = \begin{bmatrix} 1/L_{eq} & 0 & 0 \\ 0 & 1/L_{eq} & 0 \\ 0 & 0 & 1/L_{eq} \end{bmatrix} \cdot \left[\begin{bmatrix} V_{an} \\ V_{bn} \\ V_{cn} \end{bmatrix} - \begin{bmatrix} R & 0 & 0 \\ 0 & R & 0 \\ 0 & 0 & R \end{bmatrix} \begin{bmatrix} i_a \\ i_b \\ i_c \end{bmatrix} - \begin{bmatrix} e_a \\ e_b \\ e_c \end{bmatrix} \right] \tag{16}$$

The mechanical part is expressed by the following equation:

$$J \frac{d\Omega}{dt} + B\Omega = T_e - T_r \tag{17}$$

$$\frac{d\Omega}{dt} = (T_e - T_r - B\Omega)/J \tag{18}$$

with: Te : electromagnetic torque.
Tr : Load torque
Ω speed
J: moment of inertia.
B : viscose friction coefficient.

Neglecting the frictional coefficient and taking $\Omega = \frac{\omega}{p}$, where p is the pole pairs number, (18) can written as :

$$\frac{d\omega}{dt} = P.(C_e - C_r)/J \tag{19}$$

The developed torque can be expressed by

$$T_e = (e_a i_a + e_b i_b + e_c i_c)/\omega \tag{20}$$

and the angular position is expressed by

$$\frac{d\theta}{dt} = \omega \tag{21}$$

IV. HYSTERESIS CURRENT CONTROLLER (BANG-BANG CONTROL)

Several techniques can be used to control the phase current of the brushless PM DC motor. In this paper a hysteresis current controller is used. It has the major advantage of not requiring the machine parameters to be known. However the commutation frequency is not constant. [20,21,26,27]. It depends on many factors such as the applied voltage, the back emf, hysteresis band ΔI…etc.

The maximum value of frequency is obtained at starting and is given by [28] :

$$f_{\max} = U/8L_s\Delta I \tag{22}$$

The commutations are obtained by comparing actual currents $i_{a,b,c}$ to a rectangular reference $i^*_{a,b,c}$ and by keeping them in an hysteresis band ΔI., Fig.7, [20-21]
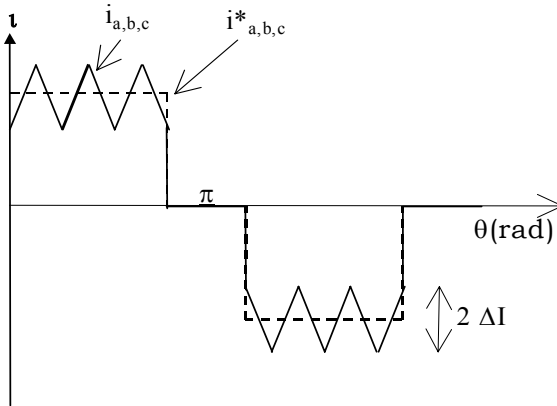

Fig.7: Rectangular hysteresis current control

The commutation sequences are summarised in the following table, Tab.1.

Table1: Commutation sequences of the switches

If $i_a < (i_a^* - \Delta I)$	T_1 on	T_4 off	$V_a = U/2$
If $i_a > (i_a^* + \Delta I)$	T_1 off	T_4 on	$V_a = -U/2$
If $i_b < (i_b^* - \Delta I)$	T_2 on	T_5 off	$V_b = U/2$
If $i_b > (i_b^* + \Delta I)$	T_2 off	T_5 on	$V_b = -U/2$
If $i_c < (i_c^* - \Delta I)$	T_3 on	T_6 off	$V_c = U/2$
If $i_c > (i_c^* + \Delta I)$	T_3 off	T_6 on	$V_c = -U/2$

Table.2 summarises all the six possible operating sequences of the motor including the phase voltages , back emf and reference currents for the hysteresis current controller.

For speed regulation, a PI controller is used. The proportional and integral gains are set to their optimal values with a critical damping ratio ξ=1

Table2: Operating Sequences of the brushless PM DC motor.

Rotor position θ°	Phase voltages, back emf and reference current values								
	V_{ao}	e_a	i_a^*	V_{bo}	e_b	i_b^*	V_{co}	e_c	i_c^*
0°-60°	U/2	$K_e\omega$	I^*	-U/2	$-K_e\omega$	$-I^*$	0	$-6K_e\omega\theta/\pi + K_e\omega$	0
60°-120°	U/2	$K_e\omega$	I^*	0	$6K_e\omega\theta/\pi - 3K_e\omega$	0	-U/2	$-K_e\omega$	$-I^*$
120°-180°	0	$-6K_e\omega\theta/\pi +5K_e\omega$	0	U/2	$K_e\omega$	I^*	-U/2	$-K_e\omega$	$-I^*$
180°-240°	U/2	$-K_e\omega$	$-I^*$	U/2	$K_e\omega$	I^*	0	$-6K_e\omega\theta/\pi + 7K_e\omega$	0
240°-300°	U/2	$-K_e\omega$	$-I^*$	0	$-6K_e\omega\theta/\pi + 9K_e\omega$	0	U/2	$K_e\omega$	I^*
300°-360°	0	$6K_e\omega\theta/\pi - 11K_e\omega$	0	U/2	$-K_e\omega$	$-I^*$	U/2	$K_e\omega$	I^*

V. PUMP MODEL.

The pump used is of centrifugal type which can be described by an aerodynamic load and is characterised by the following equation:

$$T_1 = A.\omega^2 \tag{23}$$

where A is the pump constant.

The pump mechanical characteristic is shown in Fig.8 together with the canalisation characteristic. The head versus capacity H=f (Q) characteristics are shown for the pump for different speed values using the base speed data and the affinity laws, Fig.9.
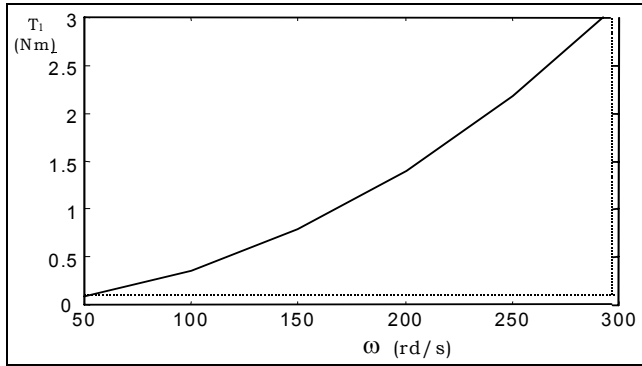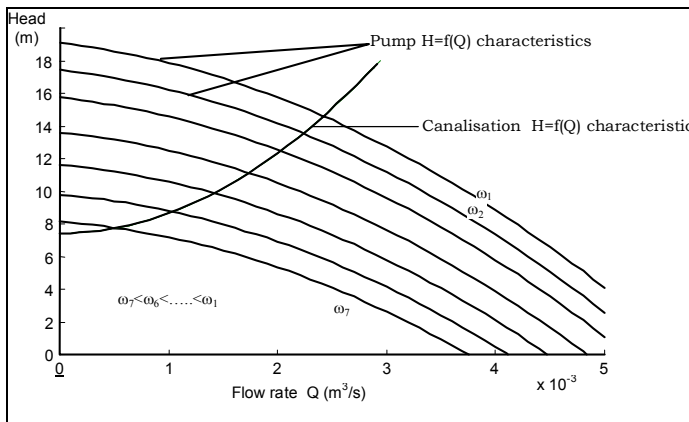
Fig.8: Pump shaft torque versus speed

Fig.9 : Multispeed family of pump head capacity curves showing operating points and canalisation characteristic.

VI. SIMULATION RESULTS

Using fourth order Runge-Kutta numerical resolution method under Matlab, the overall system shown in Fig.10 was simulated. The system was first simulated without the hysteresis current controller and PI speed regulator and then using them in order to see the effectiveness of this controller. Fig.11:a-c shows the simulation results without regulation, The phase current and torque high ripples are clearly seen. The torque pulsation are more than 15% of the average value. The source current is highly discontinuous and the speed presents an overshot in addition to its moderate response.
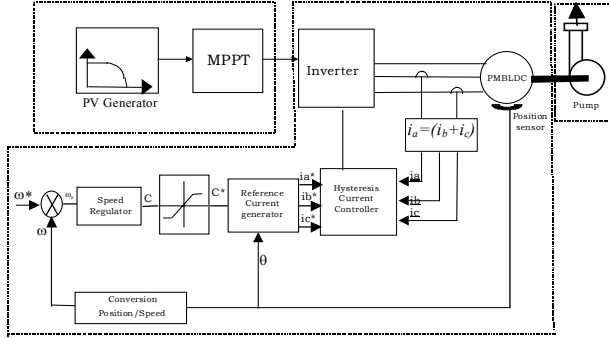
Fig.10: Overall system configuration

a) Phase Current
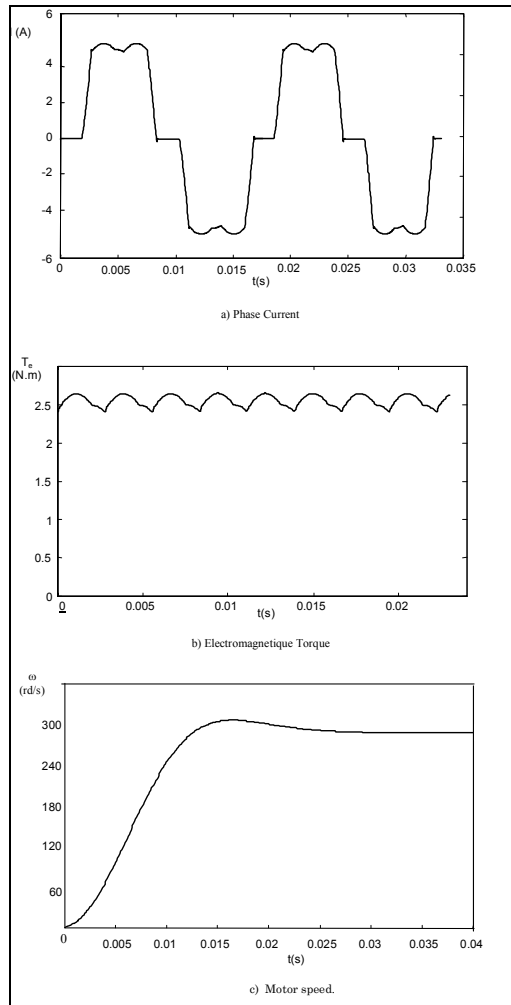
b) Electromagnetique Torque

c) Motor speed.

Fig.11: Simulation results without regulation

After, the speed and current regulations are introduced, results are shown in Fig.12. The current and torque ripples are distinctly reduced. The current oscillation are around 0.1A and the speed of response is improved with no overshot.
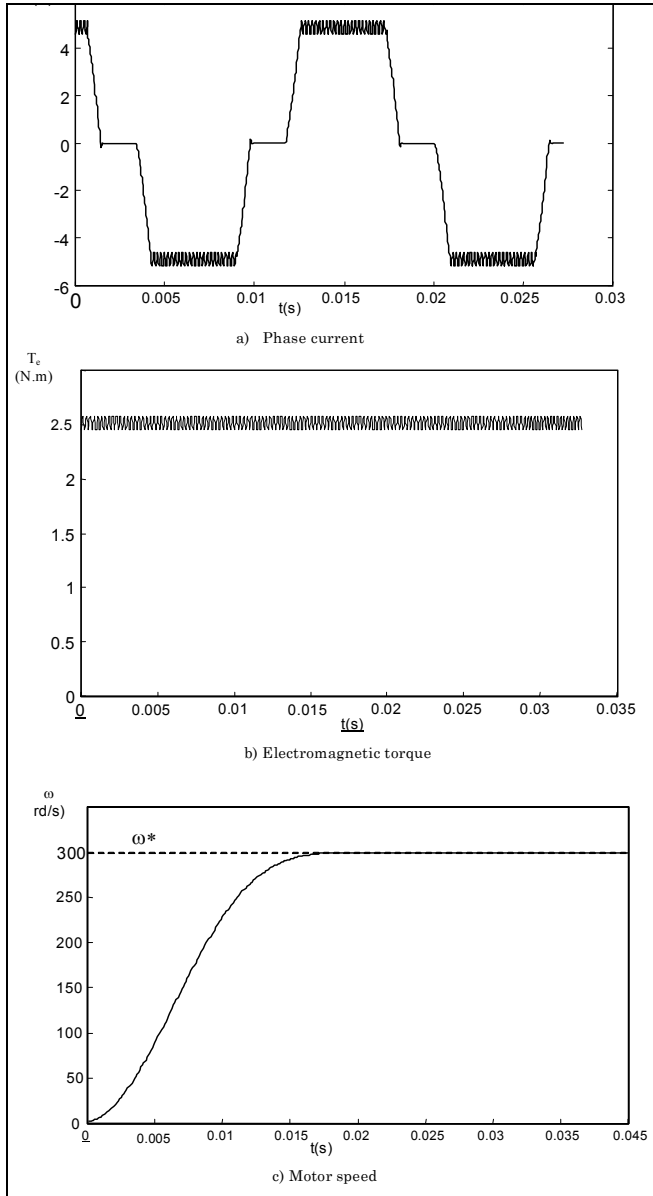
a) Phase current

b) Electromagnetic torque

c) Motor speed

Fig.12: Simulation results with PI speed and hysteresis current controllers regulation

Fig.13 show the PV generator I-V and P-V characteristics, the generator output current, the drive speed and the motor torque for a solar insolation of 1000W/m^2. It is seen that the maximum power is efficiently tracked, and the motor performances are quiet good. At starting, the current rises to the short circuit value of 4.82A with a time constant which depends on motor electrical parameters and decreases as the motor starts to run to stabilise at the value of 4.41A corresponding to the optimal current and optimal voltage of 175V. The corresponding maximum power of the PV generator is 772W. The final steady state speed of 314 rad/s is reached with no overshot.

a) Generator I-V and P-VCharacteristic

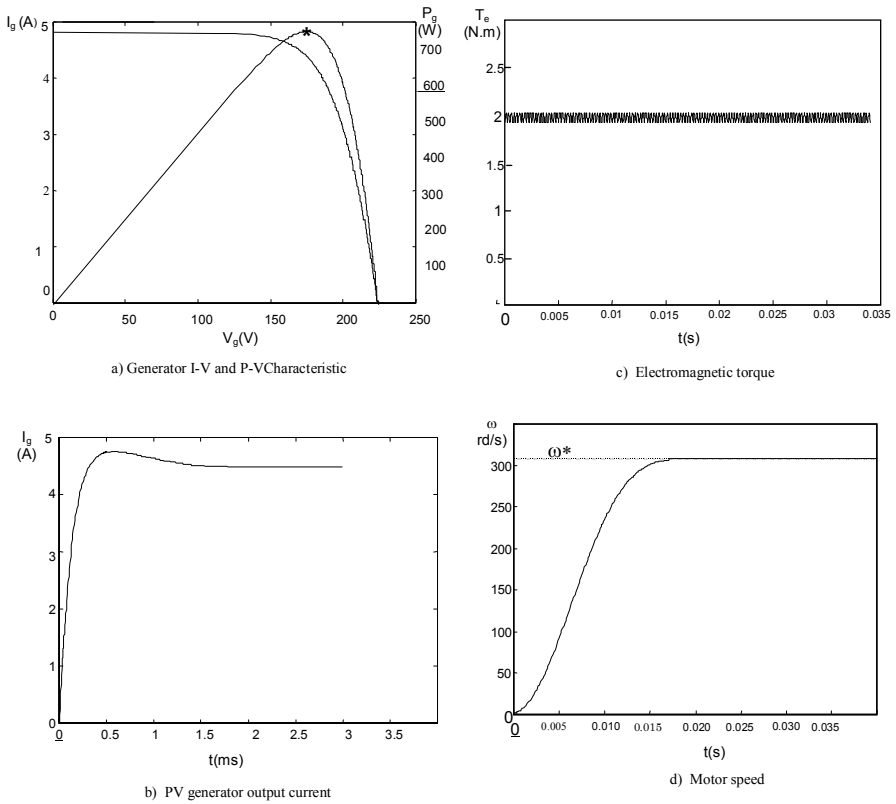c) Electromagnetic torque

b) PV generator output current

d) Motor speed

Fig.13: Simulation results for solar insolation E=1000W/m^2

Fig.14 is similar to the previous one but for a solar insolation of $500W/m^2$. In this case the current rises at a value of 2.41A and then settles down to 2.17A corresponding to the optimal current. The optimal voltage is about 170V and the maximum power is 373W. The steady state speed is 270rad/s

a Generator I-V Charactéristique

c) Electromagnetic torque

b) PV generator output current

d) Motor speed

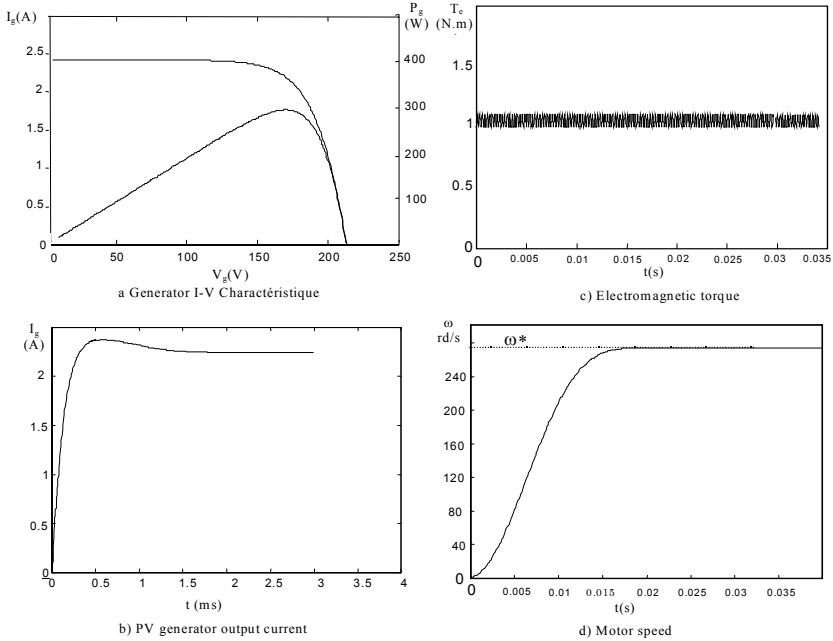*Fig.14: Simulation results for solar insolation E=500W/m²*

VII. CONCLUSION

Performances of a brushless PM DC motor connected to a photovoltaic array and driving a centrifugal pump is investigated. A hysteresis current controller and a standard PI speed controller were used. Optimal operation of the PV generator was insured by an MMPT. Simulation results showed the effectiveness of the proposed controller giving maximum power efficiency , reduced torque ripple and better speed response of the motor.

REFERENCES

LAWRANCE E. MURR ''Solar Materials Science'', Academic Press, 1980

G. B. SHRERTHA, L. GOEL, '' A Study On Optimal Sizing Of Stand Alone Photovoltaic Stations'' IEEE Trans. on EC, Vol. 13, No. 4, 1998, pp: 373-377

M. G. JABORI, '' A contribution to the Simulation and Design Optimisation of Photovoltaic Systems'' IEEE Trans. on EC, Vol. 6, No. 3, 1991, pp: 401-406

J. SAMIN and al. ''Optimal sizing of Photovoltaic Systems in Varied Climates'' Solar Energy , vol. 6, No. 2, 1997, pp: 97-107

K. KALAITZAKIS ''Optimal PV System Dimensioning with Obstructed Solar Radiation'' Renewable Energy, Vol. 7, No. 1, pp: 51-56.

Z. ZINGE, ``Optimum Operation of a Combined System pf a Solar Cell Array and a DC Motor`` , IEEE Trans. on PAS, Vol. PAS-100, No. 3, 1981, pp: 1193-1197.

J. APPELBAUM, ``Starting and Steady State Characteristics of DC Motor Powered by Solar Cell Generator`` , IEEE Trans. on EC, Vol. 1, No. 1, 1986, pp: 17-25.

M. M. SAIED, ``Matching of DC Motor to Photovoltaic generator for Maximum Daily Gross Mechanical Energy `` IEEE Trans. on EC, Vol. 3, No. 3, 1988, pp: 465-471.

W. Z. FAM, M. K. BALACHANDER, `` Dynamic Performances of a DC Shunt Motor Connected to a Photovoltaic Array``, `` IEEE Trans. on EC, Vol. 3, No. 3, 1988, pp: 613-617.

J. Appelbaum, M. S. Sarme, ``The Operation of Permanent Magnet DC motors Powered by a Common Source of Solar Cells ``, IEEE Trans. on EC, Vol. 4, No. 4, 1989, pp: 635-642.

S. M. ALGHUWAINEM, ``Steady State Operation Of DC Motors Supplied From Photovoltaic Generators With Step Up Converters`` IEEE Trans. on EC, Vol. 7, 1992, pp: 267-271.

S. SINGER, ``Starting Characteristics Of Direct Current Motors Powered By Solar Cells``, IEEE Trans. on EC, Vol. 8, No. 1, 1993, pp: 47-52.

M. AKBABA, and al. ``Matching Of Separately Excited Dc Motors To Photovoltaic Generators For Maximum Power Output``, Solar Energy, Vol. 63, N0. 6, 1998, pp:375-385

V. C. MUMMADI, ``Steady State And Dynamic Performances Analysis Of PV Supplied DC Motors Fed From Intermediate Power Converter``, Solar Energy Materials & Solar Cells, Vol-61, 2000, pp: 365-381

J. R. POTEBAUM,`` Optimal Characteristics Of A Variable Frequency Centrifugal Pump Motor Drive`` IEEE Trans. Ind. Appl., vol. IA-20, N. 1, pp. 23-31, Feb. 1984

W. R. ANIS and al. ``Coupling of a Volumetric Pump to a Photovoltaic Array``, Solar Cells, Vol. 14, PP. 27-42, 1985

O. OLORUNFEMI, ``Analyses Of Current Source Induction Motor Drive Fed From Photovoltaic Energy Source``, `` IEEE Trans. on EC, Vol. 6, No. 1, 1991, pp: 99-106

S. R. BHAT, and al, ``Performance Optimisation of Induction Motor-Pump System Using Photovoltaic Energy Source``, `` IEEE Trans. on IA, Vol. 23, No. 6, 1987, pp: 995-1000..

M. N. ESKANDAR, A. M. ZAKI, ``A Maximum Efficiency Photovoltaic-Induction Motor Pump System``, Renewable Energy, Vol. 10, No. 1, 1997, pp: 53-60

M. VEERACHARY, N. YADAIAH, ``ANN Based Peak Power Tracking For PV Supplied Dc Motors``, Solar Energy, Vol. 69, N0. 4, 2000, pp: 343-350

T. HIYAMA, and al. ``Identification Of Optimal Operating Point Of PV Modules Using Neural Network For Real Time Maximum Power Tracking Control`` IEEE Trans. on EC, Vol. 10, No. 2, 1995, pp: 360-367

T. HIYAMA, and al. ``Evaluation Of Neural Network Based Real Time Maximum Power Tracking Control For PV System`` IEEE Trans. on EC, Vol. 10, No. 3, 1995, pp: 543-548

T. HIYAMA, and al. `` Neural Network Based Estimation Of Maximum Power Generation From PV Modules Using Environmental Information`` IEEE Trans. on EC, Vol. 12, No. 3, 1997, pp: 241-247

M. GODOY, N. N. FRANCESCHETTI, ``Fuzzy Optimisation based Control of a Solar Array System`` IEE Proc. EPA, Vol. 146, No. 5, 1999, pp: 552-558

T. F. WU and al. ``A Fuzzy-Logic-Controlled Single-Stage Converter for PV-Powered Lighting System Application`` IEEE Trans. IE, Vol. 47, No. 2, 2000, pp: 287-296

H. M. MASHALY and al. ''A Photovoltaic Maximum power Tracking Using Neural Networks'' Proc of the Third IEEE Conf. On Cont. Appl. , Vol. 1, 1994, pp: 167-172

L.MERWE, G. MERWE, ''Maximum Power Point tracking-Implementation Strategies'' ISIE'98

T. SENJYU, K. UEZATO, ''Maximum Power Point Tracker Using Fuzzy Control for Photovoltaic Arrays'', Proc. of the IEEE International Conference on Industrial Technology, 1994 , pp: 143–147

I. GLASNER , J. APPELBAUM . " Advantage Of Boost Vs.Buck Topology For Maximum Power Point Tracker In Photovoltaic Systems". Tel-Aviv University, Faculty of Engineering, Dept.of Electrical Engineering-systems, Israel, IEEE.1996, pp355-358 .

I. H. ALTAS, A.M. SHARAF, ''A novel On-Line MPP Search Algorithm for PV Arrays'' IEEE Trans. on EC, Vol. 11, No. 4, 1996, pp: 748-754

D. C. MARTINS and al. ''Water Pumping System from Photovoltaic Cells Using a Current Fed Parallel Resonant Push-Pull Inverter''. 29th Annual IEEE Power Electronics Specialists Conference, 1998. PESC 98 Record, Volume: 2 , 1998, pp: 1892 -1898

C. HUA, C. SHEN, ''Study of Maximum Power Tracking Techniques and Control of DC/DC Converters for Photovoltaic Power System'' 29th Annual IEEE Power Electronics Specialists Conference, 1998. , Volume: 1 , 1998 pp: 86 – 93

C. L. P. SWAMY and al. `` Dynamic Performance of a permanent Magnet Brushless DC Motor Powered by a PV Array for Water Pumping`` Solar Energy Materials and Solar Cells, Vol. 36, 1995, pp: 187-200

APPENDIX

The PV generator, motor and pump used in this study have the following parameters:
PV generator Modules AEG-40.
(For a Temperature T=25°C and solar insolation E=1000W/m².)

Open circuit voltage	22.40 V
Short circuit current	2.410 A
Series resistance	0.450 Ω
Current temperature coefficient	0.06%/°C
Voltage temperature coefficient	0.40%/°C

Centrifugal pump

Rated speed	3000 rev/min
Rated power	521 W
Flowrate	2.597 l/s
Head	14.11 m
Efficiency	69%

Brushless DC motor

Rated power	690 W
Rated speed	3000 rev/min
Rated voltage	200-220V
Rated current	4.8 A
Per phase resistance	1 Ω
Per phase inductance	5 mH
Poles number	6
E.m.f constant	0.47